ITC 2/55
Information Technology and Control
Vol. 55 / No. 2/ 2026
pp. 838-857
DOI 10.5755/j01.itc.55.2.43472

Motion Energy Management Optimization and Health Monitoring Based on TENG Wearable Terminal

Received 2025/10/31 | Accepted after revision 2026/03/10

HOW TO CITE: Xu, J., An, D. (2026) Motion Energy Management Optimization and Health Monitoring Based on TENG Wearable Terminal. *Information Technology and Control*, 55(2), 838-857. https://doi.org/10.5755/j01.itc.55.2.43472

Motion Energy Management Optimization and Health Monitoring Based on TENG Wearable Terminal

Jixiang Xu, Di An*
College of General Education, Dongguan City University, Dongguan 523419, China

Corresponding author: Ad697850@163.com

Wearable health monitoring technology is rapidly developing and showing great potential in sports rehabilitation, chronic disease management, and personalized medicine. However, existing methods generally rely on traditional batteries, which have problems such as insufficient energy supply, poor monitoring continuity, and insufficient accuracy in identifying complex health states. Therefore, the research proposes a motion energy management optimization and health monitoring method based on Triboelectric Nanogenerator (TENG) wearable terminals, which achieves efficient acquisition, stable conversion, and adaptive scheduling of low-frequency human motion energy through a composite TENG structure and power management circuit. It also combines multi-source physiological signal preprocessing and deep learning models to enhance health status recognition capabilities. In experimental testing, the average output power of the composite TENG at 3.0Hz reached 1057.20μW, with an end-to-end efficiency of up to 88.90%, significantly better than that of the control circuit. The signal preprocessing module improved the signal-to-noise ratio to 15.47dB and the classification accuracy to 0.937. The deep learning model had a recognition accuracy of 0.936, a robustness index of only 5.80%, and could operate stably for 18.60h under energy limited conditions, with an average power consumption of only 4.80mW. This proves that the proposed method can achieve low-power, long-term, and high reliability closed-loop integrated health monitoring, providing new ideas for sustainable wearable systems.

KEYWORDS: TENG; Motion energy management optimization; Wearable health monitoring; Deep learning; Energy adaptive

1. Introduction

The rapid development of wearable electronic devices and Internet of Things (IoT) technology has greatly changed the human-computer interaction mode and daily lifestyle, providing unprecedented opportunities for continuous and real-time health monitoring and personalized exercise management [27]. However, the dependence of these devices on traditional batteries has brought a series of challenges such as limited battery life, frequent charging, increased device weight, and environmental burden [8]. Therefore, how to efficiently manage the energy obtained from human movement and how to accurately and continuously monitor health parameters are crucial for the popularization and sustainable development of wearable technology in the fields of motion and medical health [5, 14]. However, existing energy harvesting methods generally face low energy conversion efficiency caused by low frequency, irregularity, and diversity of human motion, making it difficult to meet the power consumption requirements of complex wearable functions [20, 1]. Traditional health monitoring methods are limited by the complexity of manual observation, the lag of periodic evaluation, or the limitations of high-power sensor systems in continuous and non-invasive use, especially in remote monitoring and real-time feedback, which are often hindered by insufficient power supply and the complexity of sensor integration [2, 19]. Meanwhile, existing systems still face issues such as signal interference, insufficient accuracy in identifying specific activities, and lack of self-powered continuous operation capability when extracting meaningful health insights and providing actionable recommendations. Therefore, the research optimizes exercise energy management and health monitoring based on Triboelectric Nanogenerator (TENG) wearable terminals. At the energy level, a composite TENG and power management circuit are designed to efficiently collect, stably convert, and adaptively schedule low-frequency irregular human motion energy, ensuring continuous operation of the terminal. At the monitoring level, a multi-source physiological signal acquisition and preprocessing module is constructed to synchronously collect and standardize multi-modal data such as Electrocardiogram (ECG), Electrodermal Activity (EDA), Photoplethysmography (PPG), body temperature, and blood oxygen. Meanwhile, deep learning convolution and attention mechanisms are introduced to intelligently identify health indicators. The research aims to build a low-power, long-range, self-powered closed-loop integrated wearable system, providing sustainable solutions for motion energy management and health monitoring.

2. Related Works

With the rapid development of the IoT, artificial intelligence, and flexible electronic technology, smart wearable devices have become a cutting-edge research direction in the fields of health monitoring, motion science, and personalized medicine [10, 11]. Therefore, more scholars are also conducting research, committed to solving its core challenges in energy supply, sensing accuracy, comfort, and system integration. Li et al. proposed a motion activity health monitoring device and virtual system based on IoT assistance to address the challenges posed by traditional motion health monitoring and IoT devices. The system collected real-time interactive key health information through virtualized wearable devices, effectively monitored students' motion behavior, and enhanced their physical and mental health benefits [7]. Zhang et al. proposed a flexible single electrode TENG based on multi-walled carbon nanotubes/polydimethylsiloxane film to meet the demand for lightweight, low-cost, high flexibility, and high efficiency in modern portable energy. This generator collected mechanical energy from biological movements and effectively detected human motion as a sensor, thereby achieving multi-point distributed detection and wireless data transmission for portable intelligent terminals [30]. Xu et al. proposed a new method for human behavior monitoring using friction nanogenerator sensors for intelligent IoT health management, targeting the impact of prolonged sitting, insufficient sleep, and lack of exercise on human health. This method achieved personalized motion monitoring through a single frictional nanogenerator sensor for intelligent insoles, constructed a health management system, and improved the ability to analyze and display individual health status [9]. Ding et al. proposed an autonomous continuous sweat sensing system integrated into fingertips to address the limitations of current wearable health monitoring systems on energy supply, sensing capabilities, circuit regulation, and volume. The system utilized a wearable microgrid with self-voltage regulation based on enzyme biofuel cells and silver zinc chloride batteries to obtain and store bioenergy from sweat, and continuously supply sweat through permeation [25].

In addition, Wu et al. proposed an IoT real-time health monitoring system based on deep learning to address the evolving needs of remote healthcare in the context of the IoT, as well as the challenges of protecting athletes' lives and monitoring physiological indicators in real-time. The system utilized wearable medical devices to measure vital signs and combined deep learning algorithms to analyze information, accurately analyzing athletes' conditions and remote medication guidance, and improving health monitoring efficiency and disease prevention capabilities [23]. Yıldırım et al. proposed a medical IoT framework based on wireless body area networks to address the urgent demand for new technologies and big data analysis in the healthcare field during the pandemic. This framework combined fog computing and cloud computing, and took diabetes prediction as an example. Through fuzzy logic decision of fog computing and machine learning algorithm of cloud computing, it realized efficient health big data analysis and diabetes prediction [28]. Saxena et al. proposed a convolutional-recurrent neural network machine learning algorithm that combined convolutional neural networks and recurrent neural networks to address the challenges of health monitoring and evaluation of three-phase induction motors under abnormal operating conditions such as three-phase faults and line to ground faults. This method achieved health monitoring and evaluation of abnormal operating conditions by tracking fault current patterns and extracting key features [17]. Talaat et al. proposed a wearable sensor based pressure monitoring algorithm and integrated electronic health monitoring system to address the potential of the IoT in the healthcare field and the demand for low-cost, automated prescriptions, and remote health monitoring. This system collected, processed, and analyzed human signals through wearable devices, thereby improving the medical service level of medical institutions [24].

In summary, existing research has made progress in TENG energy harvesting, single physiological signal monitoring, and cloud-based intelligent analysis, but it mainly focuses on single-module optimization and has not yet addressed the system-level coordination problem between motion energy management and multi-modal health monitoring. Therefore, it is necessary to construct a closed-loop architecture that deeply couples energy management and health monitoring. Furthermore, some TENG-based machine learning gait assistance or single-modal behavior recognition systems have recently emerged, but these studies mostly use TENG as a single sensor signal source, focusing on gait or motion pattern classification, and have not yet achieved the overall coupling of the energy link, sensing link, and health identification link. Their system structure still belongs to a linear "energy harvesting or sensing-recognition" process, which is difficult to support the continuous monitoring needs of multi-modal health indicators.

Therefore, this research proposes a method for optimizing motion energy management and health monitoring based on a motion-driven TENG wearable terminal. This method achieves efficient energy harvesting, stable conversion, and adaptive scheduling through a composite TENG structure and power management circuit, and combines multi-source physiological signal fusion and deep learning models to enable the system to intelligently identify complex health indicators such as arrhythmias, psychological stress, and emotional states. The innovation of this method lies in deeply coupling motion energy management and health monitoring, surpassing traditional TENG-based single-function sensing or behavior recognition modes, and constructing a closed-loop integrated architecture of "energy adaptive supply – multi-modal signal acquisition – intelligent health identification," providing a new systematic path for low-power, long-term, and highly reliable applications of wearable systems.

3. Methods and Materials

This research addresses the limitations of existing wearable health monitoring methods, such as dependence on external power sources, incomplete signal acquisition, and insufficient accuracy in complex state recognition. Based on advancements in energy harvesting and health monitoring, it proposes a method for optimizing kinetic energy management and health monitoring using a TENG-based wearable device. By constructing a composite TENG structure and power management circuit at the energy level, kinetic energy is efficiently collected and stably supplied. By combining multi-source physiological signal preprocessing and deep learning models, multi-modal data is fused and analyzed to improve the recognition accuracy of complex health indicators. A closed-loop architecture of "energy adaptive-multi-modal acquisition-intelligent recognition" is built to provide feasible solutions for low-power, long-term health monitoring.

3.1. Motion Energy Management Optimization Model of Wearable Terminals Based on TENG

The existing wearable terminal devices commonly rely on batteries for energy supply, resulting in range anxiety, limited lifespan, and rigid volume limitations, as well as low-efficiency of traditional energy harvesting technology in capturing low-frequency and non-stationary mechanical energy in the human body. Therefore, the research proposes an optimization model for motion energy management of wearable terminals based on TENG. Through the composite structure design of Soft Contact Triboelectric Nanogenerator (SC-TENG) and Three-Phase Magnetic Suspension/Levitation Electromagnetic Generator (TPS-EMG), human motion energy is efficiently and wideband captured from the source. An end-to-end autonomous energy management chain is constructed, which includes "Charge Maximum Extraction Optimization (CMEO) → L-Inductor + C-Capacitor (LC) buffer impedance matching → Low static power stable output → Intelligent scheduling based on energy situation", achieving full optimization from mechanical energy acquisition, efficient extraction, stable conversion to on-demand distribution. The optimization model for motion management of wearable terminals based on TENG is shown in Figure 1.

Figure 1 shows the optimization model of motion energy management for wearable terminals based on TENG, this model is not directly derived from a single existing publication, but rather is formed by integrating research on the working mechanism of triboelectric nanogenerators, the single-cycle maximum energy extraction strategy (CMEO), LC impedance matching methods, and self-powered wearable systems. The model consists of three parts: a composite energy harvesting unit, a power management circuit, and an energy scheduling mechanism, forming a complete self-powered closed-loop architecture. Firstly, in terms of energy harvesting, a hybrid structure combining SC-TENG and TPS-EMG is adopted to efficiently collect low-frequency

Figure 1

Optimization model for motion energy management of a wearable terminal based on TENG proposed in this study.

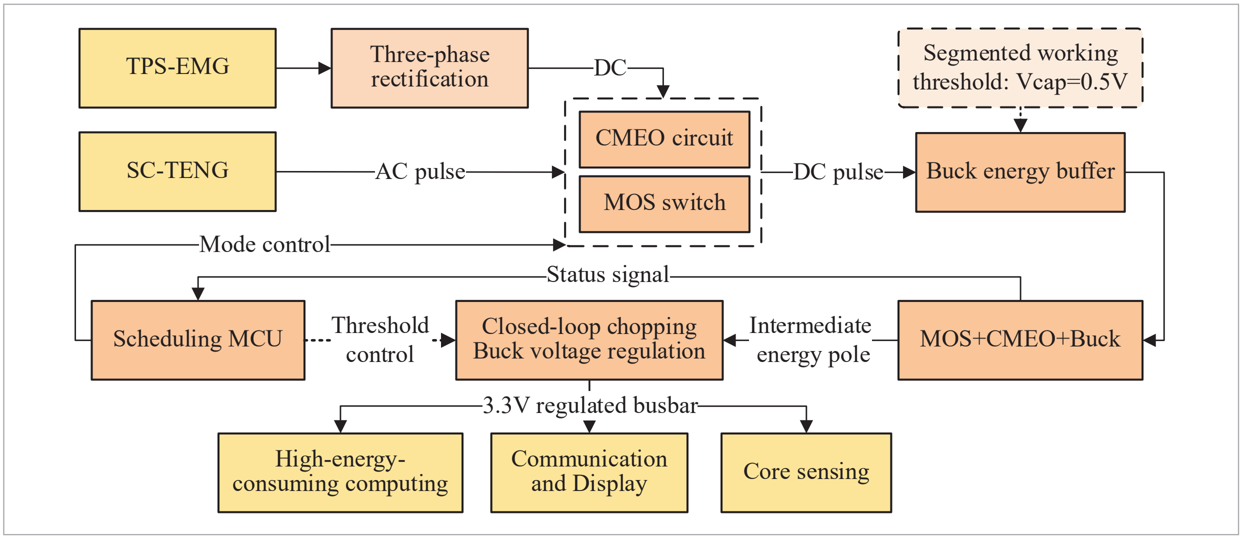

Figure 2
Wearable composite TENG structure design.

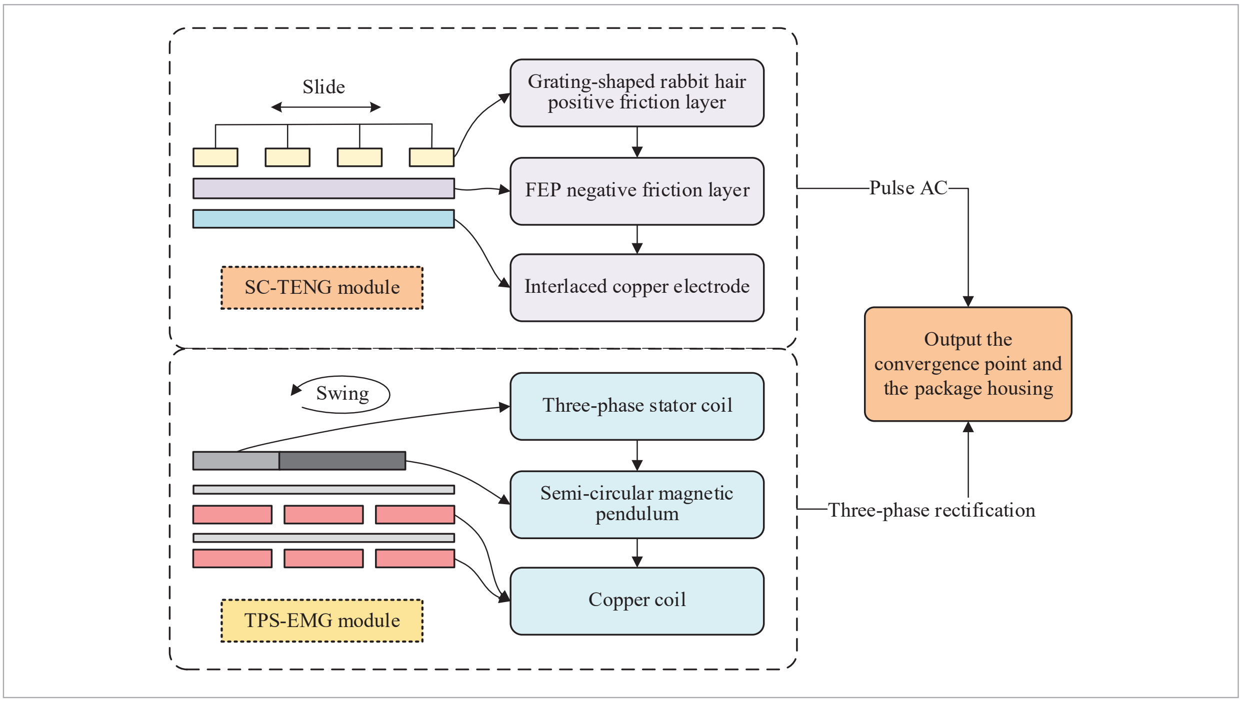

micro amplitude energy during human motion, and the durability and energy stability of the device are improved through magnetic levitation and automatic reset design. The wearable composite TENG structure design is shown in Figure 2.

Figure 2 shows the structural design of wearable composite TENG, which adopts a composite structure coupled with SC-TENG and TPS-EMG. SC-TENG works by sliding a grating like rabbit hair layer and a fluorinated ethylene propylene copolymer film on a forked electrode, significantly reducing wear through a soft contact mechanism, ensuring long-term durability ($\geq$ 20,000 cycles), and outputting high voltage, low current pulsed alternating current. The open circuit voltage of its SC-TENG is shown in Equation (1) [31, 6, 26].

$$V_{oc} = \frac{\sigma d(t)}{\varepsilon_0 S} \tag{1}$$

Equation (1) reveals the core mechanism of converting mechanical energy into electrical energy, where the open circuit voltage V_{oc} directly determines the electrical output capability. Its value is proportional to the frictional charge surface density σ and the time-varying separation distance $d(t)$, and inversely proportional to the effective contact area S. ε_0 is the vacuum dielectric constant. Equation (1) indicates that optimizing friction materials, optimizing motion structures, and designing electrode patterns are direct ways to improve the performance of SC-TENG.

TPS-EMG consists of two layers of three-phase coils and a magnetic levitation pendulum. The magnetic levitation structure provides mechanical frequency increase and automatic reset functions, which are sensitive to human bio-mechanical motion. It outputs three-phase AC power and rectifies it before outputting.

The two are integrated structurally through modular circuit board shells, complementing each other to expand the frequency band and instantaneous power of energy harvesting, jointly providing energy input for subsequent power management units.

Secondly, at the power management, an energy optimization circuit link consisting of a three-phase rectification module, a CMEO extraction module, a Buck

Figure 3

Power management circuit and energy optimization strategy of composite TENG.

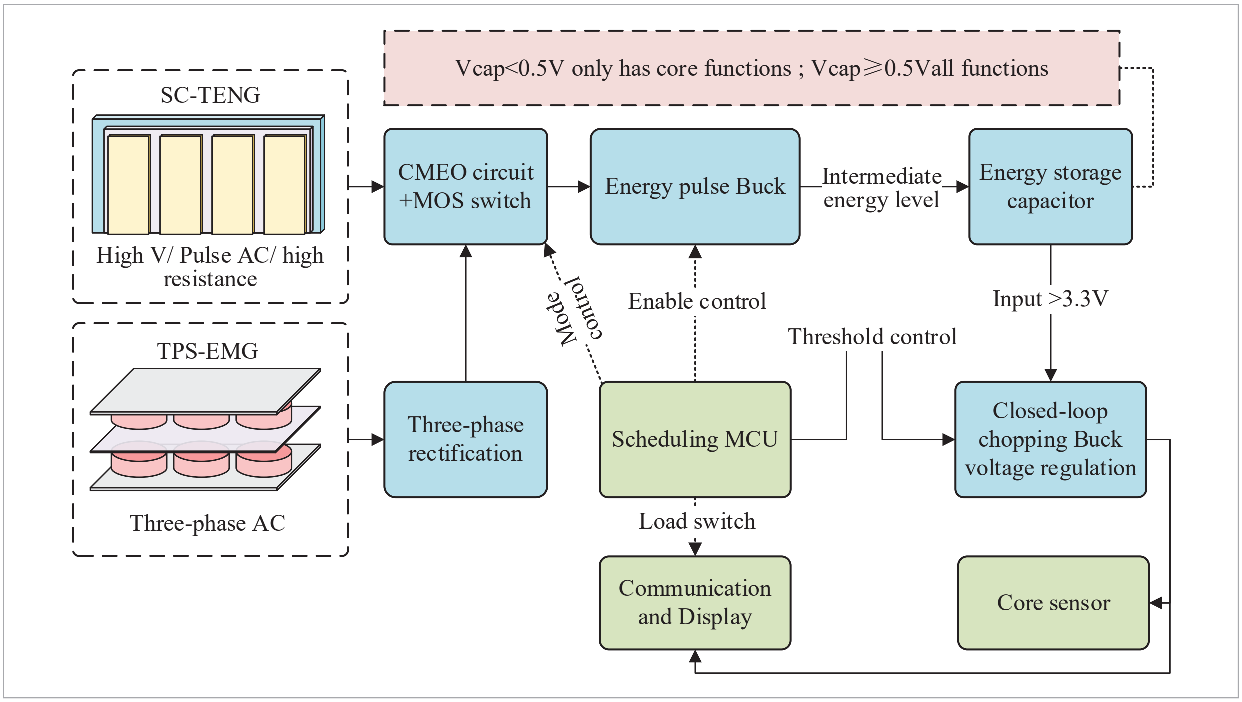

type energy buffer module, and a closed-loop chopper voltage stabilization module is designed. This not only effectively solves the high TENG output voltage, high internal resistance, and unstable signal, but also achieves single cycle energy extraction optimization through Metal-Oxide-Semiconductor (MOS) switches, improving energy conversion and storage efficiency. The power management circuit and energy optimization strategy of its composite TENG are shown in Figure 3.

Figure 3 shows the power management circuit and energy optimization strategy of the composite TENG. Firstly, the three-phase AC of TPS-EMG is rectified and converted into DC, while SC-TENG achieves efficient energy extraction through a CMEO circuit based on MOS switches, thus avoiding the drawbacks of large volume and difficult integration of traditional spark switches, as shown in Equation (2) [18, 21, 3].

$$E_{extracted} = \frac{1}{2} C_{TENG} V_{max}^2 . \tag{2}$$

Equation (2) defines the ultimate optimization objective of the power management circuit. The single cycle extracted energy $E_{extracted}$ represents the absolute upper limit of energy that can be captured from the generator, and its value is proportional to the TENG equivalent capacitance C_{TENG} (≈ 1.8nF) and the square of the peak open circuit voltage V_{max}. Equation (3) indicates that the core task of CMEO circuit is to complete energy transmission at the moment when the voltage reaches V_{max}, thereby maximizing $E_{extracted}$. Its performance is measured by approaching this theoretical value.

Secondly, after rectification and CMEO, a Buck topology containing inductance and buffer capacitor is introduced as an energy buffer unit to reduce equivalent source resistance, smooth pulses, and improve charging rate and load capacity. This indicates that the system performance is optimal when the buffer capacitor and inductance are optimally matched (such as C≈1.8 nF, L≈470μH).

A closed-loop chopper type Buck voltage regulator module is used to convert the buffered electrical energy into a stable 3.3V output. Combined with the segmented working mechanism and task priority scheduling of the capacitor voltage threshold (about 0.5V), priority power supply for key health monitoring modules and adaptive optimization of overall energy are achieved.

Finally, at the energy scheduling, dynamic power perception and priority allocation strategy are introduced to adaptively allocate energy according to the intensity of motion energy input and the importance of different sensor loads, so as to achieve stable operation of key health monitoring modules and on-demand start and stop of non-key functions, thus ensuring long-term reliable operation of wearable terminals under low power consumption conditions. The energy scheduling and system adaptation mechanism are shown in Figure 4.

Figure 4 illustrates the energy scheduling and system adaptation mechanism, aimed at addressing the intermittency and volatility of composite TENG outputs. This mechanism prioritizes terminal functions by monitoring the buffer capacitor voltage and input power status, combined with short-term energy prediction, and only guarantees core sensing tasks such as ECG and skin electrical activity when energy is insufficient. Local processing and periodic data uploading are allowed when the energy is moderate. High consumption functions such as wireless transmission and display are opened when there is excess energy or peak motion triggering. The short-term available energy prediction is shown in Equation (3) [15, 13].

$$E_{predicted}[k] = \alpha \cdot \overline{P_{in}}[k] \cdot T_{window} + (1-\alpha) \cdot E_{predicted}[k-1] \quad (3)$$

In Equation (3), the predicted energy $E_{predicted}[k]$ represents the estimated value of the available energy of the system in the k-th cycle, which is determined

Figure 4

Energy scheduling and system adaptation mechanism.

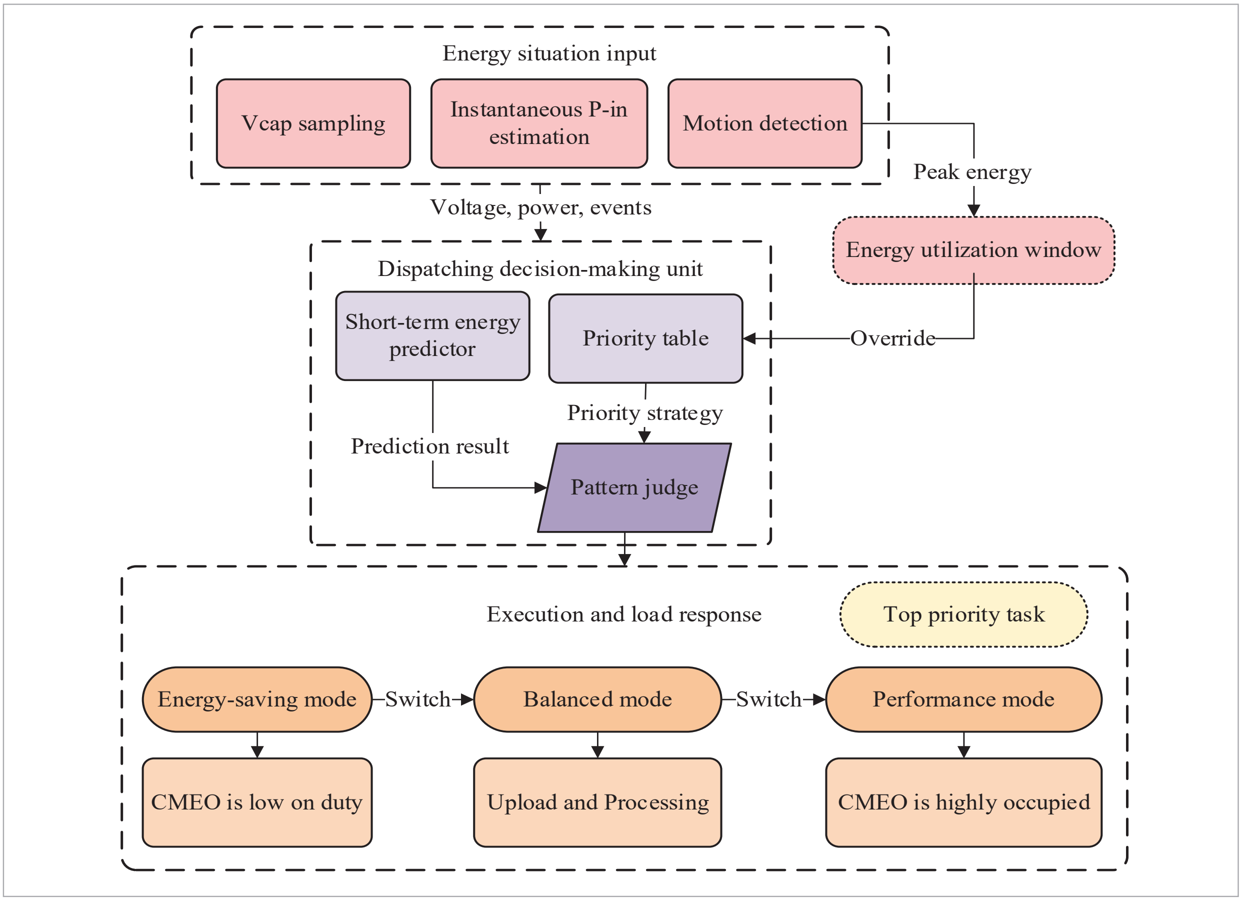

by the product of the current average input power $\bar{P}_{in}[k]$ and the predicted time window T_{window}, as well as the predicted value $E_{predicted}[k-1]$ of the previous cycle. The importance of historical information and the latest observed data is dynamically balanced through a smoothing factor α. Equation (6) concretizes the "short-term moving average" predictor in the form of an exponentially weighted moving average algorithm. This enables low-power microcontroller units to predict short-term energy trends with minimal computational overhead, providing critical data input for subsequent mode switching.

The system adopts a voltage threshold (about 0.5V) and hysteresis control to avoid frequent switching, and is coordinated by a low-power microcontroller unit to control CMEO, buffering, and voltage stabilization modules, achieving an adaptive power supply strategy of "key functions are normally on, no-key functions are started and stopped as needed", thereby improving the stability and energy efficiency utilization of wearable terminals.

3.2. Health Monitoring Method Based on Motion Energy Management Optimization Model and Deep Learning

Aiming at the high signal noise, incomplete data, and insufficient recognition accuracy of complex states in wearable health monitoring, a health monitoring method based on motion energy management optimization model and deep learning is proposed. Supported by stable energy provided by composite TENG, the integrity and temporal consistency of physiological data such as ECG, EDA, PPG, body temperature, and blood oxygen are improved through multi-source sensor fusion and unified preprocessing. Then, by combining multi-head

Figure 5

Health monitoring method based on the optimization model of exercise energy management.

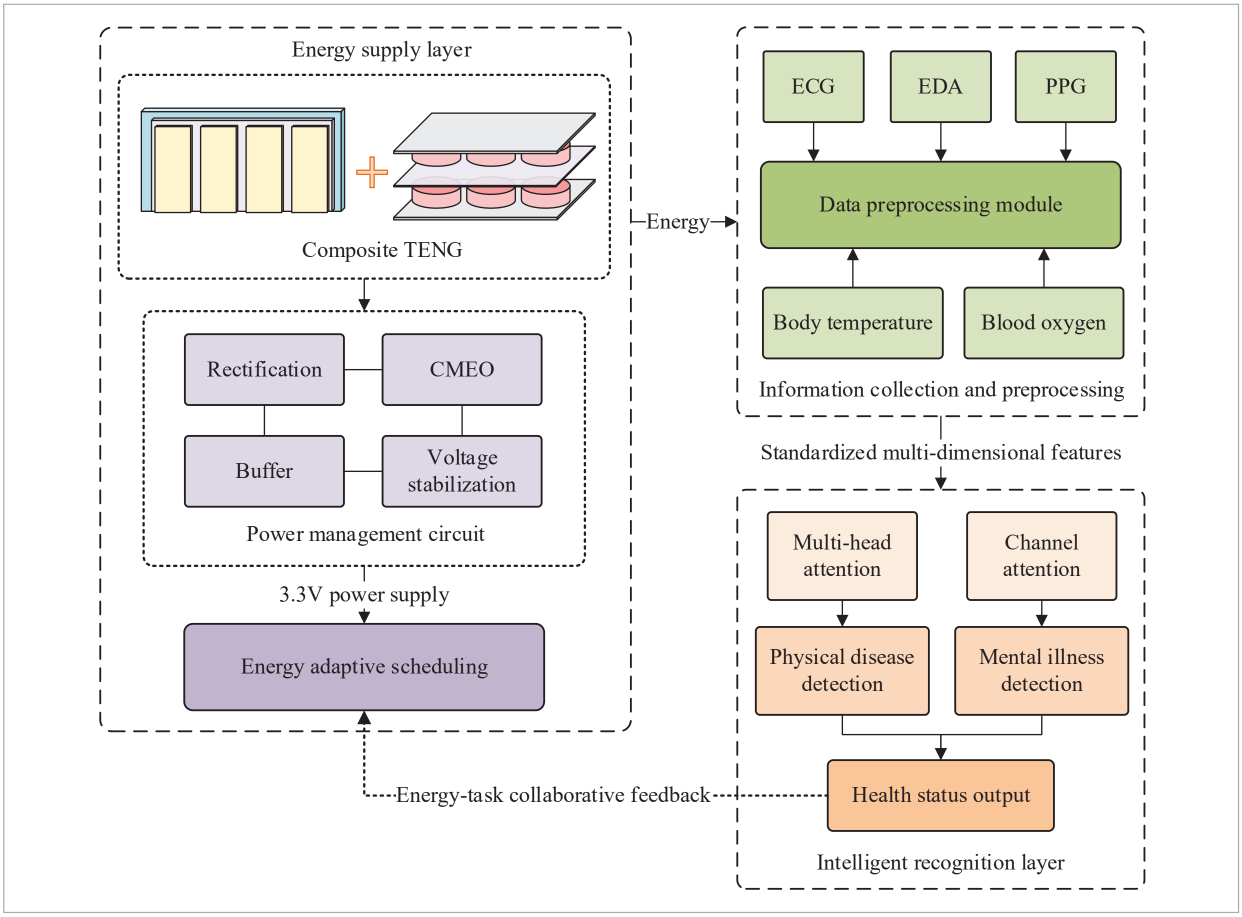

self-attention and convolutional attention mechanisms, cross-modal feature modeling is achieved, effectively enhancing the recognition accuracy and robustness of arrhythmia, psychological stress, and emotional states, thereby constructing a low-power, long-term closed-loop health monitoring system. The health monitoring method is shown in Figure 5.

Figure 5 shows the architecture diagram of a health monitoring method based on a motion energy management optimization model and deep learning. Through the integrated design of "energy supply-signal acquisition-intelligent recognition", low-power and multi-modal physiological state monitoring is achieved. Relying on the stable energy output provided by the composite TENG and power management circuit, the terminal can continuously drive multi-source sensors to collect physiological signals such as ECG, EDA, PPG, body temperature, and blood oxygen. All signals are preprocessed through unified sampling, filtering, normalization, and time alignment. The multi-source physiological signal acquisition and preprocessing module is shown in Figure 6.

Figure 6 shows the multi-source physiological signal acquisition and preprocessing module. With the energy support of the sports energy management optimization model, multi-modal health data synchronization acquisition and standardization processing have been achieved. The terminal integrates multiple types of sensors such as ECG, EDA, PPG, body temperature, and blood oxygen, and synchronously samples through a unified clock to ensure alignment and comparability of different signals in the time dimension. To address the noise, baseline drift, and missing values in the original signal, the module first uses filtering and wavelet transform for denoising and baseline correction, as shown in Equation (4) [1].

Figure 6

Multi-source physiological signal acquisition and preprocessing module.

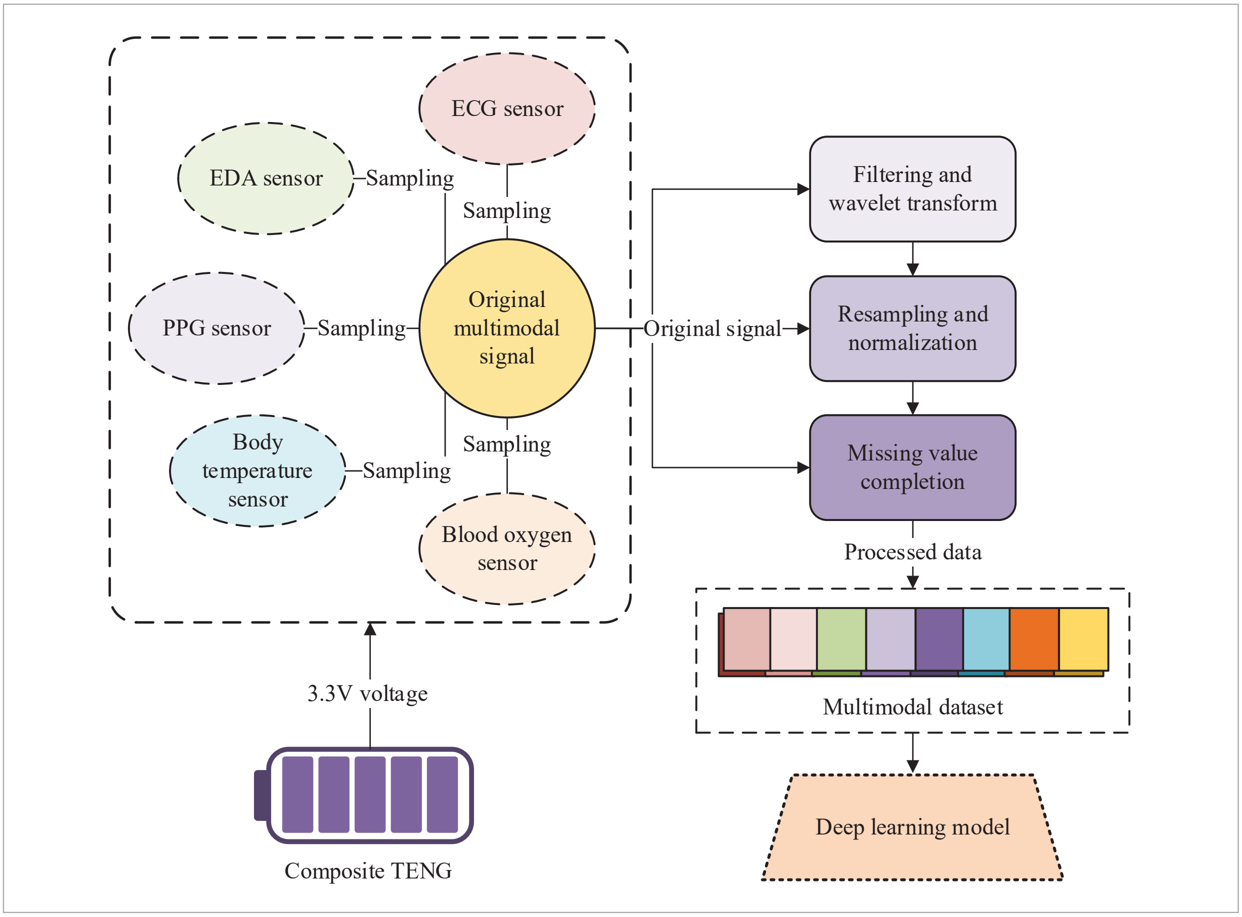

$$\begin{cases} \tilde{x}(t) = \sum_k c_{J,k}\phi_{J,k}(t) + \sum_{j=1}^{J} \sum_k d_{j,k}\psi_j, k(t) \\ d'_{j,k} = \eta_T(d_{j,k}) \end{cases} \quad (4)$$

In Equation (4), the model first decomposes the original signal $x(t)$ into approximation coefficients $c_{J,k}$ (capturing low-frequency baseline components) and detail coefficients $d_{j,k}$ (including high-frequency details and noise), where the number of decomposition layers J controls the scale depth of the processing. Subsequently, a threshold function η_T (threshold T is used to distinguish noise from effective signals) is applied to the detail coefficients. By suppressing small amplitude coefficients and retaining large amplitude coefficients, the processed coefficients $c_{J,k}$ and $d'_{j,k}$ are used to reconstruct the pure signal $\tilde{x}(t)$ after removing noise and correcting the baseline. This process synchronously solves the two major problems of high-frequency noise filtering and low-frequency baseline drift correction, and is a core mathematical tool for processing non-stationary physiological signals.

Subsequently, the time scale and amplitude range of various signals are unified through resampling and normalization methods. Finally, the interpolation and missing value completion strategy is used to generate complete and continuous multi-modal data sequences.

After processing by this module, the original irregular physiological signals are transformed into high-quality and standardized input data, providing a reliable data foundation for feature extraction and health status recognition of subsequent deep learning models.

Subsequently, the processed information is input into a deep learning model. Among them, the multi-head self-attention network is used to capture the long-range dependencies of temporal signals such as ECG, identifying arrhythmia and cardiovascular risk. The multi-channel convolution combined with attention mechanism model is used to fuse and analyze multi-modal features such as EDA and PPG for classifying and evaluating psychological stress and emotional states. With the support of energy scheduling mechanism, this method can adaptively adjust the sampling rate and model call according to the energy supply status, thereby ensuring the continuity and reliability of key health monitoring tasks under limited energy conditions. The health status recognition model based on deep learning is shown in Figure 7.

Figure 7 shows a health status recognition model based on deep learning. Firstly, a multi-channel convolutional layer is used to extract local temporal features of signals such as ECG, EDA, PPG, body temperature, and blood oxygen. The multi-scale convolution kernel is used to enhance the cross-modal feature fusion ability. Subsequently, a multi-head self-attention mechanism is introduced to model global temporal dependencies to capture long-term abnormal patterns such as arrhythmia. Its multi-head attention is shown in Equation (5) [16, 22].

$$\begin{cases} Attention(Q,K,V) = softmax(QK^T / \sqrt{d_k})V \\ MultiHead(Q,K,V) = Concat(head_1,\dots,head_h)W^O \\ where\; head_i = Attention(QW_i^Q, KW_i^K, VW_i^V) \end{cases} \quad (5)$$

In Equation (5), the multi-head self-attention mechanism equation enhances the model's ability to capture long-term relationships through a parallelization strategy. This mechanism maps input features into query matrix Q, key matrix K, and value matrix V, and calculates the scaled dot product of Q and K (divided by the square root of the key vector dimension d_k to stabilize the gradient) and normalizes it with a Softmax function to obtain attention weights. Then, V is weighted and summed to obtain a single head output $head_i$. Finally, the outputs of multiple attention heads (with a total of h) are concatenated and fused through a linear transformation matrix W^O to generate the final multi-head attention result. Among them, W_i^Q, W_i^K, and W_i^V are unique learnable parameter matrices for each head, enabling the model to pay parallel attention to long-range dependency information in different representation sub-spaces of the input sequence, thereby enhancing sensitivity to key temporal patterns.

Channel attention and temporal attention modules are overlaid on the convolutional features to highlight the modalities and key time segments that are more sensitive to psychological stress and emotional states. The channel attention module is shown in Equation (6) [29, 12].

$$\begin{cases} z_c = \frac{1}{L}\sum_{i=1}^{L} x_c(i) \\ s = \sigma(W_2\delta(W_1 z)) \\ \tilde{x}_c = s_c \cdot x_c \end{cases} \quad (6)$$

Figure 7

A health status recognition model based on deep learning.

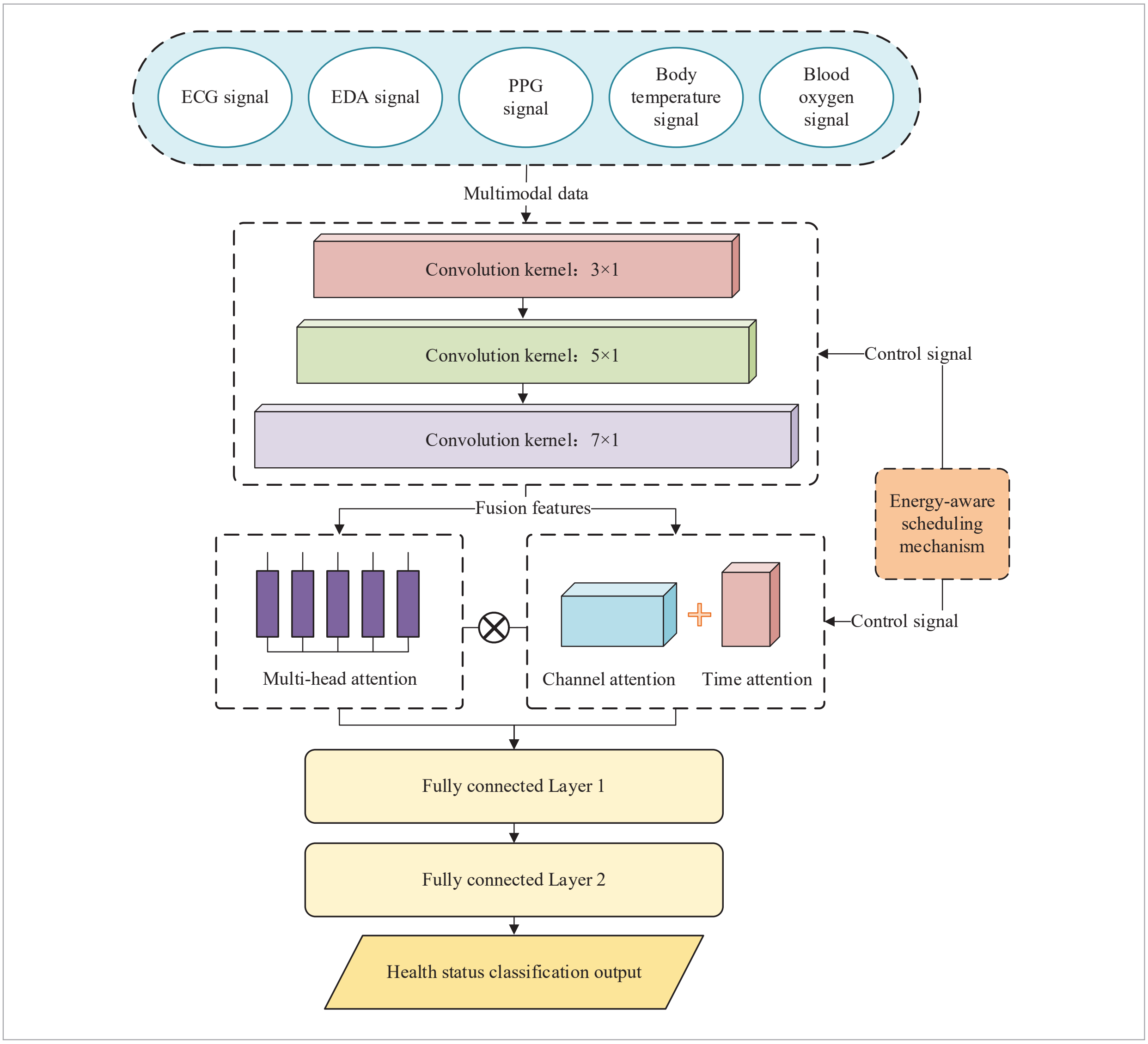

In Equation (6), the channel attention module equation adaptively fuses multi-modal signals through feature re-weighting. This module first performs global average pooling on the features x_c of each channel to obtain channel level statistics z_c. Then, it learns inter channel correlations through a bottleneck structure composed of two fully connected layer weights W_1 and W_2 (activated by ReLU δ). Finally, the Sigmoid activation function σ generates a channel attention weight s_c between 0 and 1. This weight is multiplied with the original feature x_c to obtain a re-calibrated feature $\tilde{x}c$, which enables the model to automatically strengthen the modes that contribute significantly to the current task and weaken unimportant modes, adaptively optimizing and integrating multi-source features.

Finally, the multi-task classification and risk assessment of health status are completed through the fully connected layer, intelligently recognizing cardiovascular risk, stress levels, and emotional states. The overall model works in conjunction with the energy management mechanism, balancing recognition accuracy and real-time performance while ensuring low-power operation.

Table 1

Nomenclature of key symbols used in this study.

Symbol	Description
TENG	Triboelectric Nanogenerator
SC-TENG	Soft-Contact Triboelectric Nanogenerator
TPS-EMG	Three-Phase Magnetic Suspension Electromagnetic Generator
TPS-EMG	Three-Phase Magnetic Suspension Electromagnetic Generator
V_{oc}	Open-circuit output voltage of the TENG
V_{max}	Peak output voltage of the TENG within a single cycle
C_{TENG}	Equivalent capacitance of the TENG
$E_{extracted}$	Maximum extractable energy per cycle
CMEO	Charge Maximum Extraction Optimization
$E_{preticted}$	Predicted short-term available energy
ECG	Electrocardiogram
EDA	Electrodermal Activity
PPG	Photoplethysmography

For ease of reading, the main symbols used in this study and their physical meanings are summarized in Table 1.

4. Results

4.1. Verification of Motion Energy Management Optimization for Composite TENG Wearable Terminals

To verify the reliability of the motion energy management optimization and health monitoring method based on the motion TENG wearable terminal, experimental performance verification and analysis are conducted. Firstly, the optimized motion energy management based on TENG wearable terminals is verified. An experiment platform is built and a complete energy harvesting and management performance testing process is designed. The experimental environment simulates human motion using a linear push-pull platform (frequency 0.1-5Hz, amplitude 0.5-10cm) and drives composite energy harvesting units (SC-TENG and TPS-EMG). The output signal is processed by three-phase rectification, CMEO circuit, LC buffer, and Buck voltage stabilization circuit, and finally supplies power to the load module. The signal acquisition uses Keysight DSOX2024A oscilloscope and Yokogawa WT310 power analyzer, with a sampling rate of not less than 100kHz, to accurately record pulse waveform and transient power. The experimental procedure is as follows: first, drive TENG/EMG at different frequencies and amplitudes, and record its original output characteristics. Subsequently, three control circuits (direct rectification, rectification+capacitor energy storage, traditional Buck stabilization) and the proposed experimental circuit are sequentially connected to compare the output voltage stability, energy extraction efficiency, impedance matching performance, end-to-end power transmission efficiency, and load availability. Finally, combined with energy scheduling strategies, the continuous operation capability of key health monitoring sensors is verified in the event of insufficient energy supply.

The experiment first conducts tests on energy output and power management effectiveness, selecting SC-TENG unit+bridge rectifier, TPS-EMG unit+bridge rectifier, and SC+TPS parallel connection+rectifier as controls. The test bench drives WHG with different amplitudes (maintaining amplitude/frequency correlation), records Voc/Isc (oscilloscope), single cycle energy (through integrated power or charge meter), and frequency spectrum (FFT). Each frequency point is repeated 5 times to take the average. The experimental results are shown in Figure 8.

According to Figure 8, under 3.0Hz driving, the average output power of the proposed composite TENG reached 1,057.20μW, which was 1011.30μW and 741.60μW higher than that of SC-TENG (45.90μW) and TPS-EMG (315.60μW), respectively. In the single-cycle energy test, the composite TENG reached 352.40μJ, with an increase of 226.60μJ compared to the 125.80μJ of SC+TPS parallel connection, and an increase of 247.20μJ compared to the 105.20μJ of TPS-EMG. Moreover, all frequency points showed a synchronous increase in power and energy with the increase of driving frequency, proving that the composite structure and complete power management strategy improved energy capture and conversion efficiency. Next, extraction efficiency and end-to-end efficiency tests were conducted. For each external

Figure 8

Single-cycle energy and average power depend on the driving frequency.

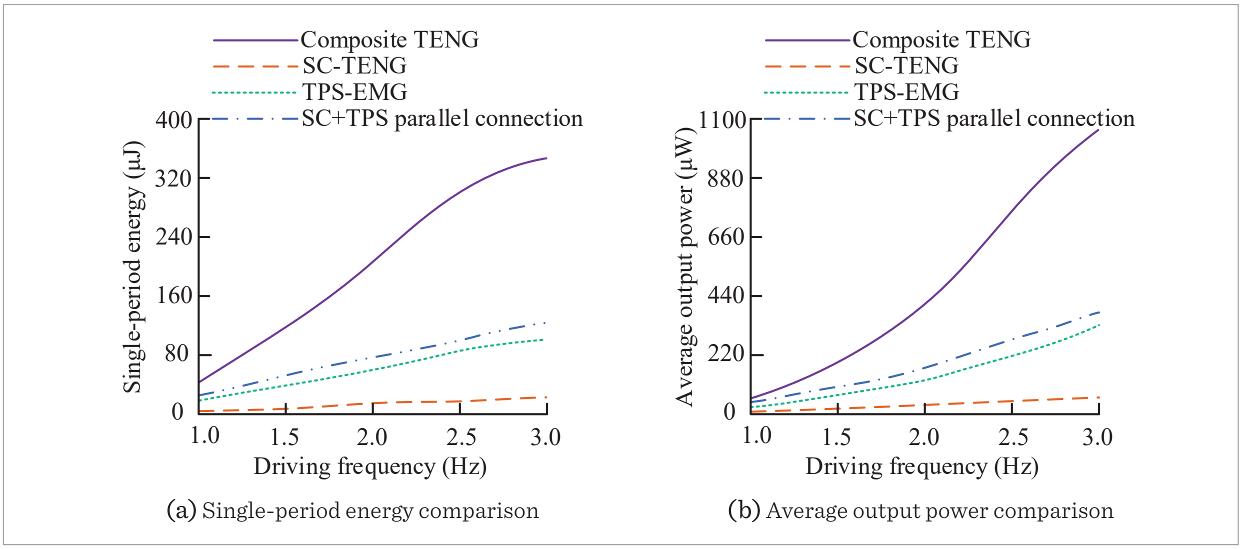

Figure 9

The variation of terminal extraction efficiency and end-to-end efficiency with load impedance.

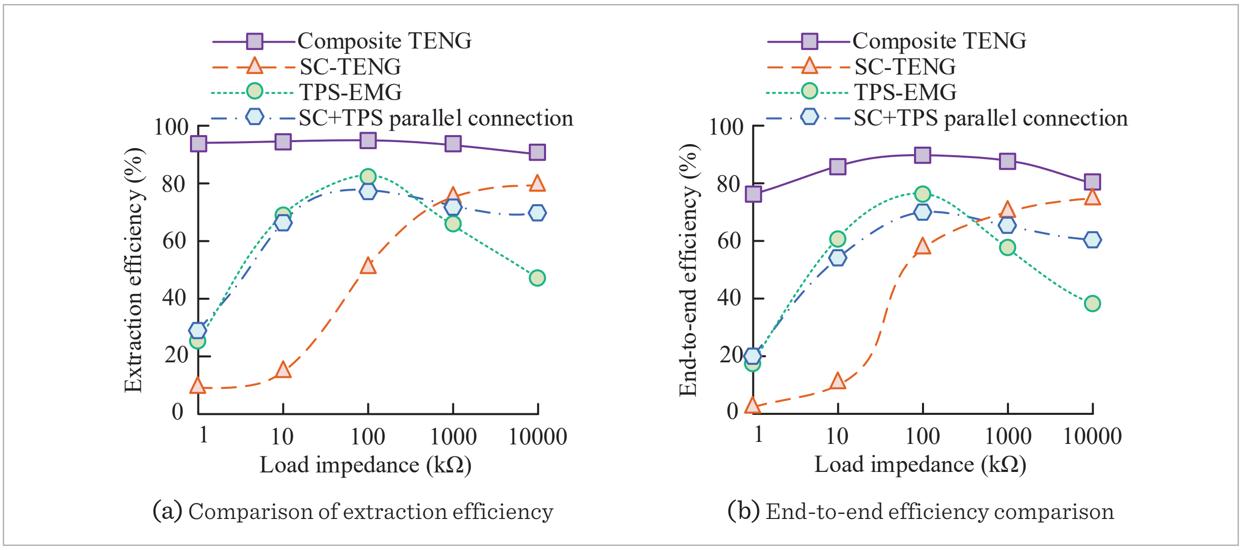

load impedance, the open circuit voltage was measured under standard driving conditions, and then the energy extraction efficiency and system end-to-end efficiency of each group were measured separately. Each point is repeated 5 times. The control group is the same as above, and its experimental results are shown in Figure 9.

According to Figure 9, under a low impedance load of 1kΩ, the end-to-end efficiency of the composite TENG was 78.50%, which was 58.35% higher than the 20.15% of SC+TPS parallel connection, 60% higher than the 18.50% of TPS-EMG, and 76.40% higher than the 2.10% of SC-TENG. Moreover, the extraction efficiency of composite TENG reached 95.20%, which was 66.50% higher than the 28.70% of SC+TPS parallel connection and 86.70% higher than the 8.50% of SC-TENG. The end-to-end efficiency of the experimental group reached a peak of 88.90%

at 100kΩ, proving that the complete power management strategy optimizes energy extraction and conversion efficiency in a wide load range.

Next, the impact of buffer parameter scanning on energy transmission and steady-state capability is tested, with composite TENG+CMEO and only composite TENG selected as controls. Th fixed drive is f=1.5Hz, various indicators are tested at different buffer parameter points. The presence/absence of CMEO is compared and each point is repeated 5 times. The experimental results are shown in Figure 10.

From Figure 10, under the optimal buffer parameter (2.0nF), the energy transmission efficiency of the complete composite TENG reached a peak of 89.67%, and the voltage stabilization duration was as long as 1,320 minutes. Compared with the composite TENG+buffer, the efficiency was improved by 30.77% and the duration was extended by 1,109.55 minutes. Compared with the composite TENG+C-MEO+buffer, the efficiency was further improved by 7.52% and the duration increased by 334.25 minutes. This fully validated the high sensitivity of system performance to buffer parameters and the effectiveness of theoretical optimal configuration.

Next, the experiment is conducted to test the system availability and critical task assurance under energy scheduling, using composite TENG, composite TENG+Dispatch, and composite TENG+Dispatch+Buffer as controls. Intermittent motion peaks (with different event rates) are simulated using controllable benches or manually manufactured sequences containing random events. The indicators of each group are recorded within 8 or 24 hours, repeating 3 times. The experimental results are shown in Figure 11.

According to Figure 11, at an input of 30 events/min, the critical task availability rate of the complete composite TENG reached 99.50%, which was 17.20% higher than that of the composite TENG+Dispatch of 82.30% and 7% higher than that of the composite TENG+Dispatch+Buffer of 92.50%. The successful upload rate reached 756.45 times/hour, 394.95 times more than the 361.50 times of single composite TENG, and 200.55 times more than the 555.90 times of composite TENG+Dispatch. Moreover, both indicators of the experimental group remained the highest at all event rates, proving that the intelligent scheduling mechanism improved the reliability and performance of the system in intermittent energy scenarios.

4.2. Validation of Health Monitoring Method Based on Motion Energy Management Optimization Model and Deep Learning

To verify the reliability and usefulness of the health monitoring method based on the kinetic energy management optimization model and deep learning,

Figure 10

The influence of buffer parameter scanning on energy transmission and steady-state capacity

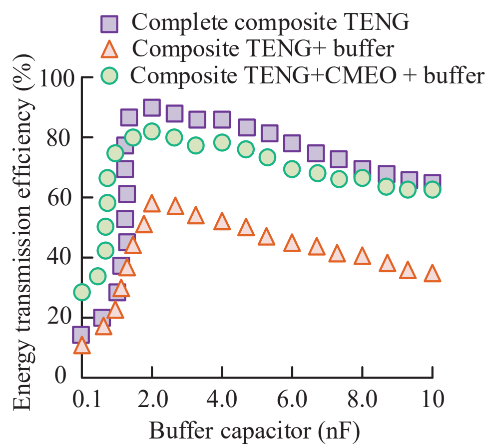

(a) Comparison of energy transmission efficiency

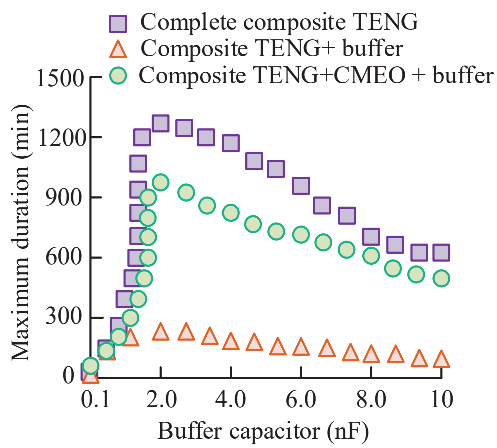

(b) Comparison of the maximum duration of power supply by the regulated busbar

Figure 11

System availability and critical mission assurance testing under energy scheduling.

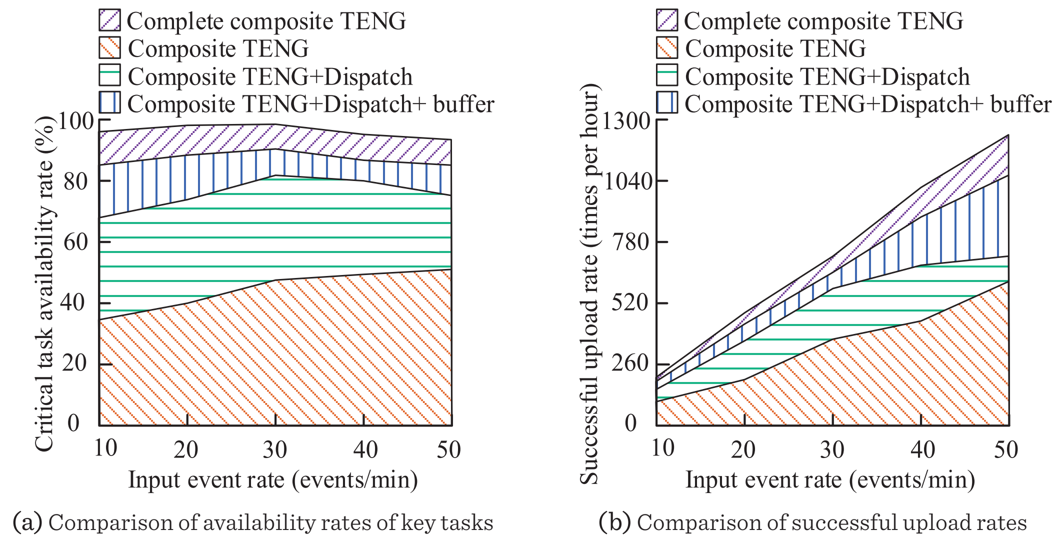

experimental performance verification and analysis were conducted. The experiment was completed under controlled laboratory conditions, using a test bench and simulated motion scenarios to perform closed-loop verification of the composite TENG energy harvesting, power management, circuit scheduling, and multimodal health monitoring processes. This was done to evaluate the system's operational stability, functional integrity, and performance limits under energy-constrained conditions. First, a unified experimental environment and system parameters were configured, and joint testing of the energy harvesting, energy management, and health monitoring modules was performed. The specific experimental environment and key parameters are shown in Table 2.

Table 2

Experimental environment and key parameters.

Experimental environment			Key configuration	
Hardware	CPU	Intel i9-11900K	Friction layer	The FEP film thickness is 50 μm network
	GPU	NVIDIA RTX 3090	Electrode Pattern	Interdigitated electrodes, period 500 μm
	RAM	32GB	Contact Pressure	0.5–1.0 N
	0torage	1TB SSD	Magnet	NdFeB, diameter 10 mm
	Operating system	Linux	Suspension Gap	1.0mm
Software	Deep learning framework	PyTorch 1.10	Batch size	128
	CUDA version	CUDA 11.x	Number of Attention Heads	8
	Python version	Python 3.8	Preprocessing	Wavelet denoising
	Dependency library	NumPy,Pandas	Dropout	0.3

Table 3
Verification of the improvement of health monitoring performance by signal preprocessing.

Evaluation dimension	Raw Signal	Filtering Preprocessing	Single-Modality Preprocessing	Health Monitoring Model
SNR Improvement (dB)	-	5.83 ± 0.87	7.25 ± 0.76	15.47 ± 0.55
Signal Completeness (%)	85.15 ± 2.33	88.92 ± 1.95	91.63 ± 1.24	98.25 ± 0.88
Time Synchronization Error (ms)	42.36 ± 3.21	25.71 ± 2.54	18.94 ± 1.98	3.82 ± 0.45
Classification Accuracy	0.72 ± 0.03	0.78 ± 0.02	0.82 ± 0.02	0.94 ± 0.01

Figure 12
Performance verification of deep learning models for complex health status recognition.

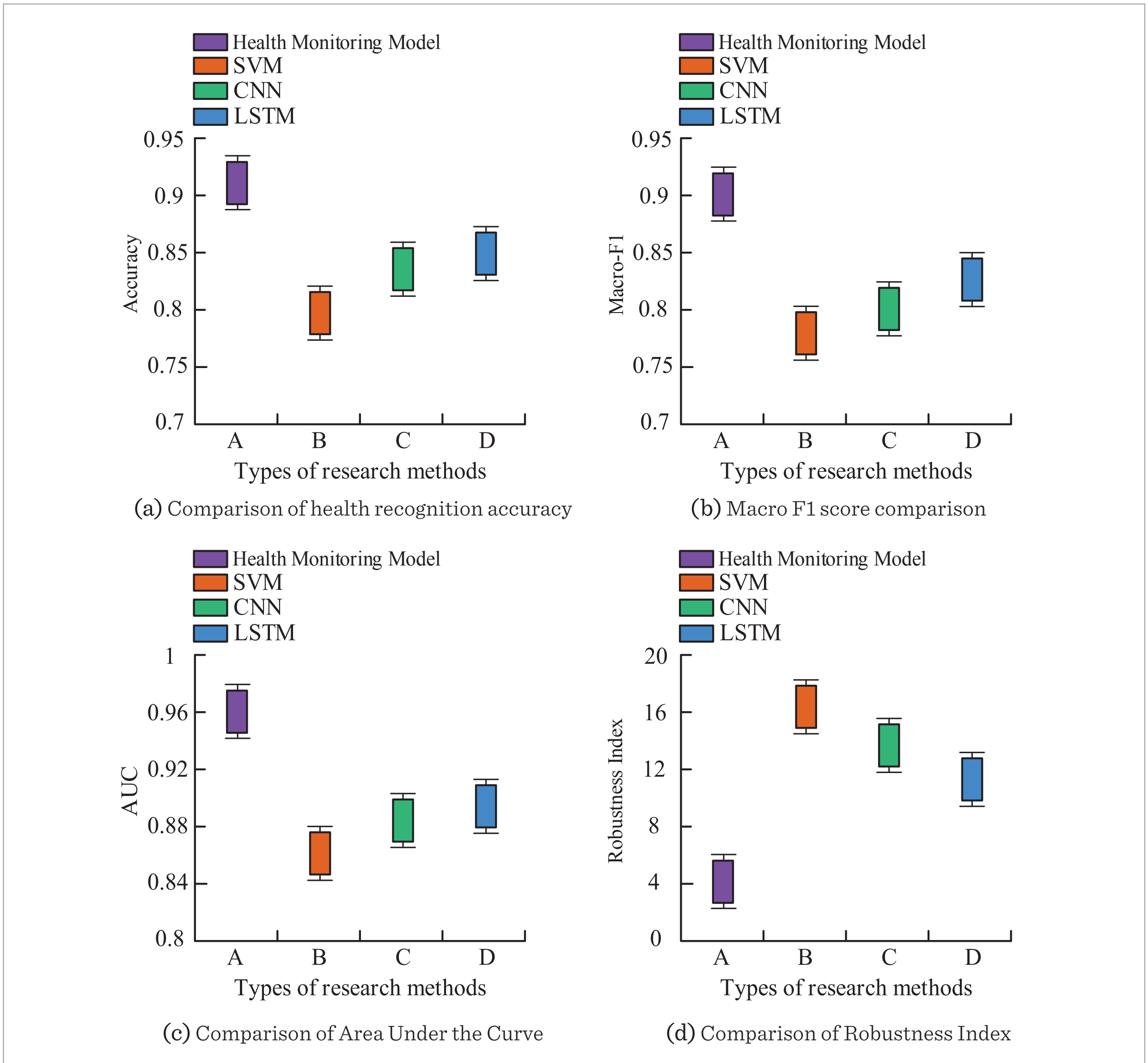

Table 2 shows the environment and key parameters of this experiment. The AMIGOS Dataset and DEAP Dataset were selected as the datasets for this experiment. Among them, the AMIGOS Dataset contains multi-modal physiological signals such as ECG, EDA, PPG, and video emotion labels, while the DEAP Dataset contains multi-channel physiological signals and annotation information based on emotional dimensions. Firstly, the experiment was conducted to verify the improvement of health monitoring performance through signal preprocessing, selecting raw data, filtering processing, and single-modality preprocessing as controls. The experimental results are shown in Table 3.

According to Table 3, the performance of the health monitoring model was superior to all control groups, with a signal-to-noise ratio (15.47dB) significantly higher than that of traditional single-mode preprocessing (7.25dB) and traditional filtering preprocessing (5.83dB). The signal completeness rate reached 98.25%, which was higher than the 91.63% of traditional single-mode preprocessing. The time synchronization error was only 3.82ms, which was significantly reduced compared to the traditional single-mode preprocessing of 18.94ms. The final classification accuracy was improved to 0.94, significantly higher than that of the traditional single-modal preprocessing (0.82), demonstrating the effectiveness of the proposed model in improving signal quality and classification performance. Next, experiments are conducted to validate the performance of deep learning models for complex health state recognition. SVM, CNN, and LSTM are selected as controls, and the experimental results are shown in Figure 12.

According to Figure 12, the comprehensive performance of the health monitoring model was the best, with significantly higher classification accuracy (0.936), macro F1 score (0.921), and AUC value (0.974) than those of LSTM (0.862, 0.843, and 0.913), single channel CNN (0.851, 0.827, and 0.901), and SVM (0.823, 0.795, and 0.879). In terms of noise robustness, the performance degradation rate of the experimental group was only 5.80%, far lower than that of the single-modal LSTM (13.20%), single-channel CNN (15.30%), and SVM (18.75%), fully demonstrating its excellent recognition ability and stability. Finally, the stability verification of the overall closed-loop architecture under energy limited conditions is conducted in the experiment, with battery-powered+SVM, battery-powered+CNN, and TENG-powered+LSTM selected as controls. The experimental results are shown in Table 4.

According to Table 4, the proposed method had the best stability under energy limited conditions, and its system stable operation time (18.60h) was significantly longer than that of TENG powered+LSTM (8.75h), battery-powered+CNN (3.20h), and battery-powered+SVM (4.50h). The effective monitoring coverage rate (77.50%) increased by 41.04% compared to TENG-powered+LSTM (36.46%). The overall recognition accuracy (0.913) was higher than that of battery-powered+CNN (0.83), battery-powered+SVM (0.78), and TENG-powered+LSTM (0.79). The average system power consumption (4.80mW) was lower than that of all control groups, especially significantly reduced compared to battery-powered systems, demonstrating its superiority in high efficiency, energy saving, and sustainable operation.

Table 4

Stability verification of the overall closed-loop architecture under energy-constrained conditions.

Evaluation dimension	Battery-powered+SVM	Battery-powered+CNN	TENG-powered+LSTM	Proposed Method
Stable Operation Time (h)	4.50 ± 0.35	3.20 ± 0.28	8.75 ± 0.82	18.60 ± 1.05
Effective Monitoring Coverage (%)	18.75 ± 1.62	13.33 ± 1.45	36.46 ± 3.21	77.50 ± 2.88
Core Task Availability (%)	95.20 ± 1.25	93.50 ± 1.42	78.30 ± 3.55	88.90 ± 1.85
Overall Accuracy	0.78 ± 0.03	0.83 ± 0.02	0.79 ± 0.03	0.91 ± 0.02
Average System Power (mW)	42.50 ± 1.85	38.90 ± 1.72	5.25 ± 0.48	4.80 ± 0.35

5. Discussion

The wearable motion-enabled energy management and health monitoring method proposed in this study demonstrates significant improvements in energy harvesting efficiency, power supply stability, and multi-modal health recognition capabilities. Compared to the flexible single-electrode TENG energy harvesting and motion monitoring system proposed by Zhang et al. [31], which possesses flexibility and wearability, its output voltage is unstable and lacks sufficient matching, making it unable to support the continuous operation of multi-modal sensors. However, this study introduces a composite structure of SC-TENG and TPS-EMG in the energy link, achieving an end-to-end efficiency of up to 88.90% through CMEO single-cycle energy maximization extraction and LC impedance matching. Xu et al.'s [26] behavior monitoring system based on a triboelectric nanogenerator insole focuses on motion behavior recognition, with a single signal dimension, making it unable to extend to complex health indicators such as arrhythmias, psychological stress, and emotional states. In contrast, this study does not rely on a single TENG signal as the basis for health monitoring, but instead uses a composite TENG to provide stable energy, driving multiple sensors such as ECG, EDA, PPG, body temperature, and blood oxygen, forming a multi-modal data fusion framework. Although the autonomous sweat sensing system based on a microgrid proposed by Ding et al. [4] achieves continuous power supply based on sweat bioenergy, its power supply link is mainly targeted at a single metabolic sensing task. In contrast, this study further proposes an energy status prediction and task priority scheduling mechanism, allowing the system to maintain stable operation of critical tasks even under energy constraints, achieving continuous monitoring for up to 18.60 hours. Wu et al.'s [25] deep learning-based IoT health monitoring system relies on external power and cloud computing, making it sensitive to energy consumption and difficult to operate autonomously for extended periods. This study uses a composite TENG to provide local energy support and achieves edge intelligent recognition through low-power design and local deep learning models, reducing reliance on external power and communication.

Although the methods presented in this study show significant improvements in energy management efficiency, monitoring coverage, and recognition accuracy, certain limitations remain. For example, the energy output of the composite TENG is still affected by exercise intensity and individual differences, which may lead to a decrease in power supply stability at very low exercise levels. The data quality of the multi-modal physiological signal acquisition module still depends on the fit of the wearable device. Although the computational load of deep learning models has been optimized, energy consumption may still increase with larger models or more complex tasks. In the future, further improvements can be achieved by combining ultra-low-power model compression techniques, flexible patch-type multimodal sensors, and efficient energy storage materials to enhance the system's adaptability and robustness across various scenarios.

6. Conclusion

A motion energy management optimization and health monitoring method based on motion TENG wearable terminal was proposed to address the unstable energy supply, disconnection between health monitoring and energy management, and insufficient accuracy in complex state recognition in wearable health monitoring systems. Through the composite TENG structure, power management circuit, and energy scheduling mechanism, efficient collection and stable supply of motion energy were achieved. Combined with multi-source physiological signal preprocessing and deep learning models, the accuracy and robustness of health monitoring were improved. The experimental results showed that the energy transmission efficiency of the research method reached 89.67% under optimized buffer parameters, and the steady-state power supply time was 1,320 minutes, far exceeding the control group, verifying the effectiveness and stability of the energy scheduling mechanism. In terms of health monitoring, the proposed signal preprocessing module improved the signal-to-noise ratio to 15.47dB, the signal integrity rate was 98.25%, and the classification accuracy was 0.937, which was superior to traditional preprocessing methods. The accuracy of the deep learning model in complex health state recognition was 0.936, with macro F1 of 0.921 and AUC of 0.974, and the robustness index was only

5.80%, which was significantly better than control models such as SVM, CNN, and LSTM. The overall closed-loop architecture operates stably for 18.60h under energy limited conditions, with an effective monitoring coverage rate of 77.50% and an average power consumption of only 4.80mW, which was superior to battery-powered or traditional models. In summary, the proposed method achieves low-power, long-term, and high reliability health monitoring through a closed-loop architecture of "energy adaptive supply-multi-modal signal acquisition-intelligent health recognition", providing a feasible path for the development of intelligent wearable systems.

Furthermore, the proposed closed-loop integrated architecture currently exists as a working laboratory prototype. Its overall performance validation is primarily based on controlled laboratory environments and simulated motion scenarios, and has not yet undergone system-level deployment testing in complex real-world wearable or long-term practical application environments. Future work will involve further long-term validation in real-world scenarios and under various user conditions to comprehensively assess the engineering feasibility and robustness of this closed-loop system in practical applications.

Conflicts of Interest

The authors declare that they have no conflicts of interest.

References

1. Abrori, S. A. Wearable Sensors for Health Monitoring: Technologies, Applications, Challenges and Future Perspectives. Engineering, Mathematics and Computer Science Journal (EMACS), 2025, 7(2), 229-239. https://doi.org/10.21512/emacsjournal.v7i2.13765
2. Alshamrani, M. IoT and Artificial Intelligence Implementations for Remote Healthcare Monitoring Systems: A Survey. Journal of King Saud University - Computer and Information Sciences, 2022, 34(8), 4687-4701. https://doi.org/10.1016/j.jksuci.2021.06.005
3. Chen, S., Qiao, Z., Niu, Y. Wearable Flexible Microfluidic Sensing Technologies. Nature Reviews Bioengineering, 2023, 1(12), 950-971. https://doi.org/10.1038/s44222-023-00094-w
4. Ding, S., Saha, T., Yin, L. A Fingertip-Wearable Microgrid System for Autonomous Energy Management and Metabolic Monitoring. Nature Electronics, 2024, 7(9), 788-799. https://doi.org/10.1038/s41928-024-01236-7
5. Feng, Z., Zhao, Z., Liu, Y. Piezoelectric Effect Polyvinylidene Fluoride (PVDF): From Energy Harvester to Smart Skin and Electronic Textiles. Advanced Materials Technologies, 2023, 8(14), 2300021-2300022. https://doi.org/10.1002/admt.202300021
6. Gao, F., Liu, C., Zhang, L. Wearable and Flexible Electrochemical Sensors for Sweat Analysis: A Review. Microsystems & Nanoengineering, 2023, 9(1), 1-2. https://doi.org/10.1038/s41378-022-00443-6
7. Gharehbaghi, V. R., Noroozinejad Farsangi, E., Noori, M. A Critical Review on Structural Health Monitoring: Definitions, Methods and Perspectives. Archives of Computational Methods in Engineering, 2022, 29(4), 2209-2235. https://doi.org/10.1007/s11831-021-09665-9
8. He, J., Cao, L., Cui, J. Flexible Energy Storage Devices to Power the Future. Advanced Materials, 2024, 36(4), 2306090-2306091. https://doi.org/10.1002/adma.202306090
9. Lee, S. W., Pei, X., Rajendran, J. A Wireless and Battery-Free Wearable Pressure Sensing System for Human-Machine Interaction and Health Monitoring. IEEE Journal on Flexible Electronics, 2023, 2(6), 439-447. https://doi.org/10.1109/JFLEX.2023.3300997
10. Li, Q., Kumar, P. M., Alazab, M. IoT-Assisted Physical Education Training Network Virtualization and Resource Management Using a Deep Reinforcement Learning System. Complex & Intelligent Systems, 2022, 8(2), 1229-1242. https://doi.org/10.1007/s40747-021-00584-7
11. Li, Z., Huang, L., Cheng, L. Laser-Induced Graphene-Based Sensors in Health Monitoring: Progress, Sensing Mechanisms and Applications. Small Methods, 2024, 8(11), 2400118-2400119. https://doi.org/10.1002/smtd.202400118
12. Mahato, K., Saha, T., Ding, S. Hybrid Multimodal Wearable Sensors for Comprehensive Health Monitoring. Nature Electronics, 2024, 7(9), 735-750. https://doi.org/10.1038/s41928-024-01247-4
13. Min, S., Kim, D. H., Joe, D. J. Clinical Validation of a Wearable Piezoelectric Blood-Pressure Sensor for

Continuous Health Monitoring. Advanced Materials, 2023, 35(26), 2301627-2301628. https://doi.org/10.1002/adma.202301627

14. Nwibor, C., Haxha, S., Ali, M. M. Remote Health Monitoring System for the Estimation of Blood Pressure, Heart Rate and Blood Oxygen Saturation Level. IEEE Sensors Journal, 2023, 23(5), 5401-5411. https://doi.org/10.1109/JSEN.2023.3235977
15. Pandey, P., Maharjan, P., Seo, M. K. Recent Progress in Wearable Triboelectric Nanogenerator for Advanced Health Monitoring and Rehabilitation. International Journal of Energy Research, 2024, 2024(1), 5572736-5572737. https://doi.org/10.1155/2024/5572736 Sarkar, A., Hossain, S. K. S., Sarkar, R. Human Activity Recognition from Sensor Data Using Spatial Attention-Aided CNN with Genetic Algorithm. Neural Computing and Applications, 2023, 35(7), 5165-5191. https://doi.org/10.1007/s00521-022-07911-0
16. Saxena, A., Kumar, R., Rawat, A. K. Abnormal Health Monitoring and Assessment of a Three-Phase Induction Motor Using a Supervised CNN-RNN-Based Machine Learning Algorithm. Mathematical Problems in Engineering, 2023, 2023(1), 1264345-1264346. https://doi.org/10.1155/2023/1264345
17. Singh, A., Chatterjee, K. Edge Computing Based Secure Health Monitoring Framework for Electronic Healthcare System. Cluster Computing, 2023, 26(2), 1205-1220. https://doi.org/10.1007/s10586-022-03717-w
18. Subramanian, K., Hajamohideen, F., Viswan, V., Shaffi, N., Mahmud, M. Exploring Intervention Techniques for Alzheimer's Disease: Conventional Methods and the Role of AI in Advancing Care. Artificial Intelligence Applications, 2024, 2(2), 59-77. https://doi.org/10.47852/bonviewAIA42022497
19. Sujith, A., Sajja, G. S., Mahalakshmi, V. Systematic Review of Smart Health Monitoring Using Deep Learning and Artificial Intelligence. Neuroscience Informatics, 2022, 2(3), 100028-100029. https://doi.org/10.1016/j.neuri.2021.100028
20. Taherdoost, H. Wearable Healthcare and Continuous Vital Sign Monitoring with IoT Integration. Computers, Materials & Continua, 2024, 81(1), 79-80. https://doi.org/10.32604/cmc.2024.054378
21. Talaat, F. M., El-Balka, R. M. Stress Monitoring Using Wearable Sensors: IoT Techniques in Medical Field. Neural Computing and Applications, 2023, 35(25), 18571-18584. https://doi.org/10.1007/s00521-023-08681-z
22. Wang, H., Li, S., Lu, H. Carbon-Based Flexible Devices for Comprehensive Health Monitoring. Small Methods, 2023, 7(2), 2201340-2201341. https://doi.org/10.1002/smtd.202201340
23. Wang, Y., Haick, H., Guo, S. Skin Bioelectronics Towards Long-Term, Continuous Health Monitoring. Chemical Society Reviews, 2022, 51(9), 3759-3793. https://doi.org/10.1039/D2CS00207H
24. Wu, X., Liu, C., Wang, L. Internet of Things-Enabled Real-Time Health Monitoring System Using Deep Learning. Neural Computing and Applications, 2023, 35(20), 14565-14576. https://doi.org/10.1007/s00521-021-06440-6
25. Xu, L., Zhong, S., Yue, T. AIoT-Enhanced Health Management System Using Soft and Stretchable Triboelectric Sensors for Human Behavior Monitoring. EcoMat, 2024, 6(5): e12448-e12449. https://doi.org/10.1002/eom2.12448
26. Yang, L., Amin, O., Shihada, B. Intelligent Wearable Systems: Opportunities and Challenges in Health and Sports. ACM Computing Surveys, 2024, 56(7), 1-42. https://doi.org/10.1145/3648469
27. Yıldırım, E., Cicioğlu, M., Çalhan, A. Fog-Cloud Architecture-Driven Internet of Medical Things Framework for Healthcare Monitoring. Medical & Biological Engineering & Computing, 2023, 61(5), 1133-1147. https://doi.org/10.1007/s11517-023-02776-4
28. Yuan, J., Zhang, Y., Wei, C. A Fully Self-Powered Wearable Leg Movement Sensing System for Human Health Monitoring. Advanced Science, 2023, 10(29), 2303114-2303115. https://doi.org/10.1016/j.measen.2024.101086
29. Zainab, H., Khan, A. H., Khan, R. Integration of AI and Wearable Devices for Continuous Cardiac Health Monitoring. International Journal of Multidisciplinary Science and Arts, 2024, 3(4), 123-139. https://doi.org/10.47709/ijmdsa
30. Zhang, H., Zhang, D. Z., Wang, D. Y. Flexible Single-Electrode Triboelectric Nanogenerator with MWCNT/PDMS Composite Film for Environmental Energy Harvesting and Human Motion Monitoring. Rare Metals, 2022, 41(9), 3117-3128. https://doi.org/10.1007/s12598-022-02031-z